Symmetry-protected trivial phases and quantum phase transitions in an anisotropic antiferromagnetic spin-1 biquadratic model

Xi-Hao Chen,[1,2] Ian McCulloch,[3] Murray T. Batchelor,[4,5,1] and Huan-Qiang Zhou[1,*]

[1]*Centre for Modern Physics, Chongqing University, Chongqing 400044, The People's Republic of China*

[2]*Research Institute for New Materials and Technology, Chongqing University of Arts and Sciences, Chongqing 400000, The Peoples Republic of China*

[3]*School of Mathematics and Physics, The University of Queensland, St. Lucia, QLD 4072, Australia*

[4]*Department of Theoretical Physics, Research School of Physics, The Australian National University, Canberra Australian Capital Territory 2601, Australia*

[5]*Mathematical Sciences Institute, The Australian National University, Canberra Australian Capital Territory 2601, Australia*

(Received 27 December 2019; revised 3 August 2020; accepted 4 August 2020; published 24 August 2020)

The ground-state phase diagram is obtained for an antiferromagnetic spin-1 anisotropic biquadratic model. With the help of symmetry and duality transformations, three symmetry-protected trivial phases and one dimerized symmetry-breaking phase are found. Local and nonlocal order parameters are identified to characterize these phases. Quantum phase transitions between the symmetry-protected phases belong to the Gaussian universality class with central charge $c = 1$, and quantum phase transitions from the symmetry-protected trivial phases to the dimerized phase belong to the Ising universality class with central charge $c = 1/2$. In addition, the model admits three characteristic lines of factorized ground states, which are located in the symmetry-protected trivial phases instead of a symmetry-breaking phase, in sharp contrast to other known cases.

DOI: 10.1103/PhysRevB.102.085146

I. INTRODUCTION

Much attention has been focused on critical phenomena in quantum many-body systems with an aim towards a complete classification of quantum states of matter. In this regard, significant progress has been made for quantum spin systems in one dimension, resulting in the introduction of novel concepts, such as symmetry-protected topological order [1] and symmetry-protected trivial (SPt) order [2]. A SPt phase is a symmetric phase connected adiabatically to a product state and is characterized in terms of a nonlocal order parameter defined by the combined operation of the site-centered inversion symmetry with a π rotation around the z axis in the spin space. As a consequence, such a SPt phase is different from a symmetry-protected topological phase [1]. Therefore, it is expected to also play an important role in classifying quantum states of matter [2,3]. However, it remains unclear whether or not the current characterization of SPt phases in terms of the nonlocal order parameter is generic enough for any possible SPt phases.

On the other hand, dualities, symmetries, and factorized ground states combine to play a significant role in characterizing physical properties for quantum many-body systems [4]. An intriguing question is how then to demonstrate the powerfulness of all these concepts in one single illustrative example. In this paper, we investigate the nature of SPt phases appearing in the ground-state phase diagram for an anisotropic generalization of the spin-1 biquadratic model [5,6], which is known to be in a dimerized phase. The more general model proposed here is described by the Hamiltonian,

$$H = -\sum_{i=-\infty}^{\infty} \left(J_x S_i^x S_{i+1}^x + J_y S_i^y S_{i+1}^y + J_z S_i^z S_{i+1}^z\right)^2, \qquad (1)$$

where S_i^α ($\alpha = x,\ y$ and z) denote spin-1 operators at site i on an infinite-size chain with J_x, J_y, and J_z the spin couplings describing the interactions among the x, y, and z components. The model is antiferromagnetic, in the sense that it becomes the antiferromagnetic spin-1/2 XYZ model, which itself is an exactly solvable model [7], if S_i^α's are spin-1/2 operators.

The model Hamiltonian (1) reduces to the spin-1 SU(2)-invariant biquadratic model when $J_x = J_y = J_z$. The spin-1 biquadratic model has been extensively investigated. It can be either mapped to the nine-state Potts model [5] or solved directly in terms of Bethe ansatz or functional relations [6]. It is, thus, known to be in a dimerized phase with a relatively small spectral gap. The Hamiltonian (1) of the anisotropic generalization of this model commutes with the three operators $\Sigma_x = \Sigma_i(-1)^i[(s_i^y)^2 - (s_i^z)^2]$, $\Sigma_y = \Sigma_i(-1)^i[(s_i^z)^2 - (s_i^x)^2]$, and $\Sigma_z = \Sigma_i(-1)^i[(s_i^x)^2 - (s_i^y)^2]$. In particular, these three commuting operators, combining with S_i^α, generate a SU(3) symmetry when $J_x = J_y = J_z$ [8]. It is the staggered nature of the symmetry operators which explains why spontaneous dimerization occurs in the spin-1 SU(2)-invariant biquadratic model [5].

*Corresponding author: hqzhou@cqu.edu.cn

TABLE I. The six symmetry and duality transformations for the biquadratic Hamiltonian (1) defined in relation (2).

U	Spin transformation	$k(X,Y)$	X'	Y'
U_a	$S^x_{2i} \to -S^y_{2i}$, $S^y_{2i} \to -S^x_{2i}$, $S^z_{2i} \to -S^z_{2i}$, $S^x_{2i+1} \to S^y_{2i+1}$, $S^y_{2i+1} \to S^x_{2i+1}$, $S^z_{2i+1} \to -S^z_{2i+1}$	1	$-Y$	$-X$
U_b	$S^x_i \leftrightarrow S^y_i$, $S^z_i \to -S^z_i$	1	Y	X
U_1	$S^x_i \to -S^x_i$, $S^y_i \to S^z_i$, $S^z_i \to S^y_i$	Y^2	X	$1/Y$
U_2	$S^x_{2i} \to -S^x_{2i}$, $S^y_{2i} \to -S^z_{2i}$, $S^z_{2i} \to -S^y_{2i}$, $S^x_{2i+1} \to -S^x_{2i+1}$, $S^y_{2i+1} \to S^z_{2i+1}$, $S^z_{2i+1} \to S^y_{2i+1}$	Y^2	$-X/Y$	$-1/Y$
U_3	$S^x_i \to S^z_i$, $S^y_i \to -S^y_i$, $S^z_i \to S^x_i$	X^2	$1/X$	Y/X
U_4	$S^x_{2i} \to -S^z_{2i}$, $S^y_{2i} \to -S^y_{2i}$, $S^z_{2i} \to -S^x_{2i}$, $S^x_{2i+1} \to S^z_{2i+1}$, $S^y_{2i+1} \to -S^y_{2i+1}$, $S^z_{2i+1} \to S^x_{2i+1}$	X^2	$-1/X$	$-Y/X$

II. DUALITY TRANSFORMATIONS

Key information about the nature of the phase diagram can be obtained from duality relations among the spin couplings. Here, quantum duality is represented by a local unitary transformation U acting on Hamiltonian (1). For convenience and simplicity, we define the variables $X = J_x/J_z$ and $Y = J_y/J_z$ and consider $H(X,Y)$. In general, if $H(X',Y')$ is dual to $H(X,Y)$, there should exist a unitary transformation U satisfying

$$H(X,Y) = k(X,Y)UH(X',Y')U^\dagger. \tag{2}$$

The coupling parameters X' and Y' are functions of X and Y with $k(X,Y)$ being positive.

For Hamiltonian (1), there are two symmetry transformations and four duality transformations as presented in Table I. These symmetry and duality transformations imply six self-dual lines defined by $X = \pm 1$, $Y = \pm 1$, and $Y/X = \pm 1$.

III. GROUND-STATE PHASE DIAGRAM

To obtain the phase diagram, we consider the self-dual lines $J_x/J_z = 1$, $J_y/J_z = 1$, and $J_y/J_x = 1$, which delineate the six regions shown in Fig. 1(a). Because of the various symmetries and dualities, we only need to focus on one of these six regions with the whole phase diagram following by mapping with the help of the duality transformations. We, thus, define region I as the principal regime. To determine the phase boundary in region I, we examine order parameters based on numerical simulations in terms of the infinite time-evolving block decimation (iTEBD) algorithm [9] and the infinite density-matrix renormalization-group (iDMRG) algorithm [10]. In both algorithms, ground-state wave functions are represented in terms of infinite matrix product states (iMPS). We will also make use of the von Neumann entropy. Figure 1(b) shows the ground-state phase diagram determined in this way as discussed in detail below.

IV. FACTORIZED STATES

When $J_x = 0$, the system is in a factorized ground state. The wave function of this factorized state can be written as a simple product of the vector $\frac{1}{\sqrt{2}}(1,0,-1)$. The corresponding factorized energies are given by $e = -(J_y^2 + J_z^2)$. Similarly, the system is also in a factorized state when $J_y = 0$ or $J_z = 0$, respectively, as follows from the duality transformations. The wave functions can then be written as products of the vector $\frac{1}{\sqrt{2}}(1,0,1)$ or (0,1,0) with energies $e = -(J_x^2 + J_z^2)$ or $e = -(J_x^2 + J_y^2)$, respectively. These three factorized states are dual to each other. Note that, if we choose J_z as an energy scale, then, $J_z = 0$ is equivalent to saying that both J_x and J_y approach infinity with a fixed ratio J_x/J_y. We also note that, when $J_x = J_y = 0$, the model has 2^N degeneracies with entanglement varying between 0 and ∞, consistent with previous results for systems with largely degenerate ground states [11].

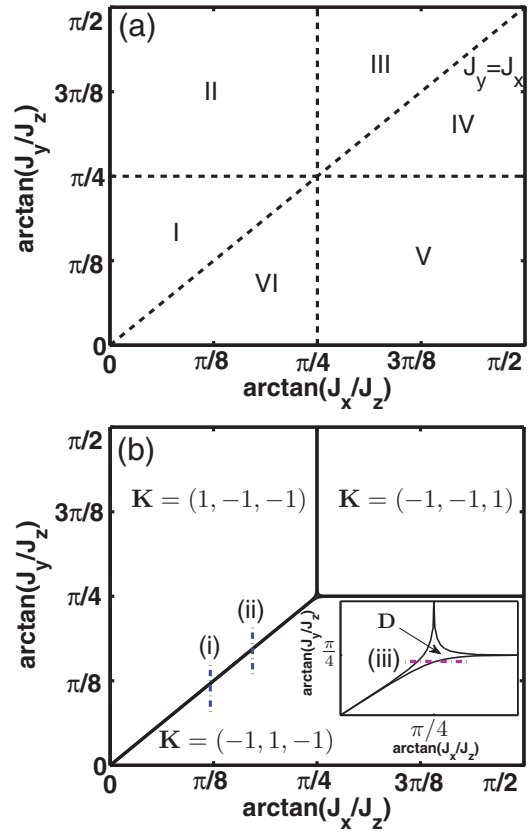

FIG. 1. (a) The six dual regions in the $J_x/J_z \geqslant 0$ and $J_y/J_z \geqslant 0$ parameter space of the spin-1 biquadratic anisotropic model. Region I is the principal regime. (b) The phase diagram characterized by three Z_2 combined symmetry operations $\boldsymbol{K} = (K_x, K_y, K_z)$ and order parameters $\boldsymbol{D} = (D_x, D_y, D_z)$. The inset shows a magnification of the tiny region defining the dimerized phase. The dashed-dotted paths labeled by (i)–(iii) are sample lines discussed in the text to show how to characterize these phases.

V. SYMMETRY-PROTECTED TRIVIAL PHASES

Spontaneous symmetry breaking (SSB) occurring in quantum many-body systems implies the existence of long-range order which can be characterized by local-order parameters. Significantly, there exist other concepts of order in quantum many-body systems which are beyond Landau theory due to

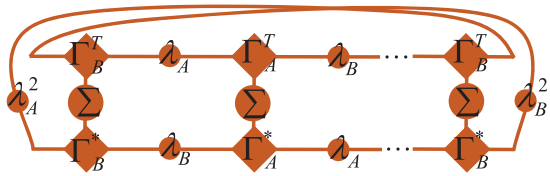

FIG. 2. Graphical representation of non-local-order parameters in the MPS picture. Γ_A and Γ_B are three-index tensors; λ_A and λ_B are Schmidt decomposition coefficients. These four tensors with a two-site translation invariance form the ground-state wave-function $|\psi\rangle$ of the infinite-size spin chain.

the absence of any SSB. Examples are the three SPt phases mentioned above, which cannot be successfully characterized by local-order parameters. Fortunately, appropriate non-local-order parameters can be used to characterize such order, which may be regarded as a natural extension of the SPt order introduced in Ref. [2]. Indeed, distinct non-local-order parameters can successfully distinguish various symmetry-protected phases and are effective for symmetry-protected gapped phases with partial symmetry breaking [12,13].

For a given ground-state wave function $|\psi\rangle$ of an infinite-size spin chain represented by the iMPS, the site-centered non-local-order parameters can be written based on reversing an odd-sized segment of the chain and, then, calculating the resulting overlap [2,14]. This can be defined in terms of the inversion operator,

$$O_L^\alpha = \frac{\langle\psi|I_{(1,L)}\Sigma^\alpha_{(1,L)}|\psi\rangle}{tr\left(\lambda_A^2\lambda_B^2\right)}, \tag{3}$$

where O_L^α is the inversion on the segment from 1 to L with internal symmetry operations $\Sigma^\alpha_{(1,L)}$ acting on the physical indices. Here, $\Sigma^\alpha_{(1,L)}$ is $\exp(i\pi S^\alpha)$ with S^α a spin-1 matrix and $\alpha = x, y,$ or z. The segment length L is odd. λ_A and λ_B are Schmidt decomposition coefficients.

This definition respects two-site translation invariance due to the fact that it can work on non-SSB and SSB wave functions directly. In the absence of SSB, O_L^α gives a ± 1 value. Conversely, O_L^α gives a 0 value for SSB. Figure 2 shows the graphical representation of non-local-order parameters in the MPS framework. Each SPt phase can then be characterized by the values of (O_L^x, O_L^y, O_L^z) of the non-local-order parameters. When L approaches the thermodynamic limit, the non-local-order parameters (O_L^x, O_L^y, O_L^z) obtain the exact values of (K_x, K_y, K_z). We denote these three Z_2 combined symmetry operations by $\boldsymbol{K} = (K_x, K_y, K_z)$.

We employ the definition of non-local-order parameters (3) on the three sample lines: (i) $J_x/J_z = 0.4$, (ii) $J_x/J_z = 0.6$, and (iii) $J_y/J_z = 0.988$ as indicated in the phase diagram Fig. 1(b). First consider lines (i) and (ii). In Fig. 3, we plot O_L^x, O_L^y, and O_L^z as functions of J_y/J_z for fixed $J_x/J_z = 0.4$ and fixed $J_x/J_z = 0.6$ with truncation dimension $\chi = 100$. Quantum phase transition (QPT) points are located at $J_x^c/J_z = 0.4$ and $J_x^c/J_z = 0.6$, respectively. Increasing the inversion block size L from $L = 101$ to $L = 201$, O_L^x reaches the saturation value of -1 most efficiently when J_y/J_z is away from the QPT point J_y^c/J_z. In contrast, O_L^x saturates much slower in the vicinity of J_y^c/J_z. The values of O_L^y and O_L^z behave similarly.

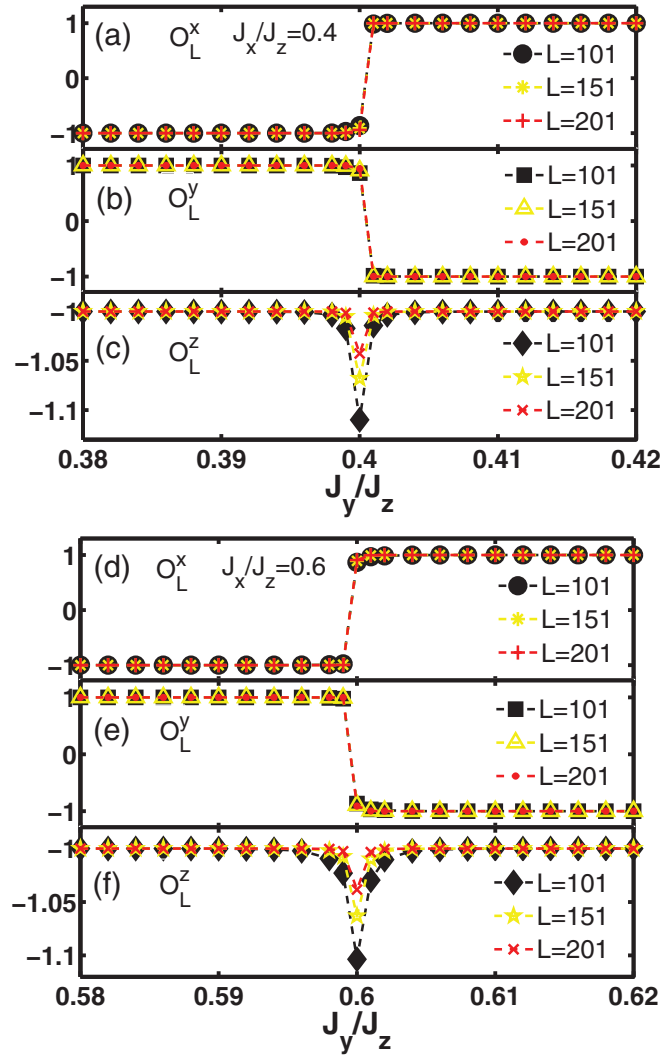

FIG. 3. Non-local-order parameters O_L^α as a function of coupling J_y/J_z with truncation dimension $\chi = 100$ for fixed $J_x/J_z = 0.4$ (top) and 0.6 (bottom). The parameter L shown is the inversion block size. QPT points are identified as $J_y^c/J_z = 0.4$ and 0.6. For each panel the symmetry parameter values of $\boldsymbol{K} = (-1, 1, -1)$ for the left side and $\boldsymbol{K} = (1, -1, -1)$ for the right side of the QPT point. The data sets correspond to lines (i) and (ii) in Fig. 1(b).

In this way, the SPt phase on the left-hand side of the QPT points J_y^c/J_z is characterized by $\boldsymbol{K} = (1, -1, -1)$, which corresponds to the SPt phase above (PA) diagonal phase boundaries. Similarly, the phase on the right-hand side of the QPT points J_y^c/J_z is characterized by $\boldsymbol{K} = (-1, 1, -1)$, which corresponds to the SPt phases below (PB) diagonal phase boundaries. Based on the dual regions in Fig. 1(a), the SPt PA phase is in region I and the SPt PB phase is in region VI. These two phases are, thus, dual to each other, separated by the self-dual line $J_y = J_x$. The values of $\boldsymbol{K} = (1, -1, -1)$ of the non-local-order parameters in region I and $\boldsymbol{K} = (-1, 1, -1)$ in region VI foretell their duality. Based on duality, one knows, e.g., that the non-local-order parameters of the SPt phase in regions III and IV can be written as $\boldsymbol{K} = (-1, -1, 1)$.

Turning to line (iii) in Fig. 1(b), we plot O_L^x, O_L^y, and O_L^z as a function of J_x/J_z for fixed $J_y/J_z = 0.988$ with truncation

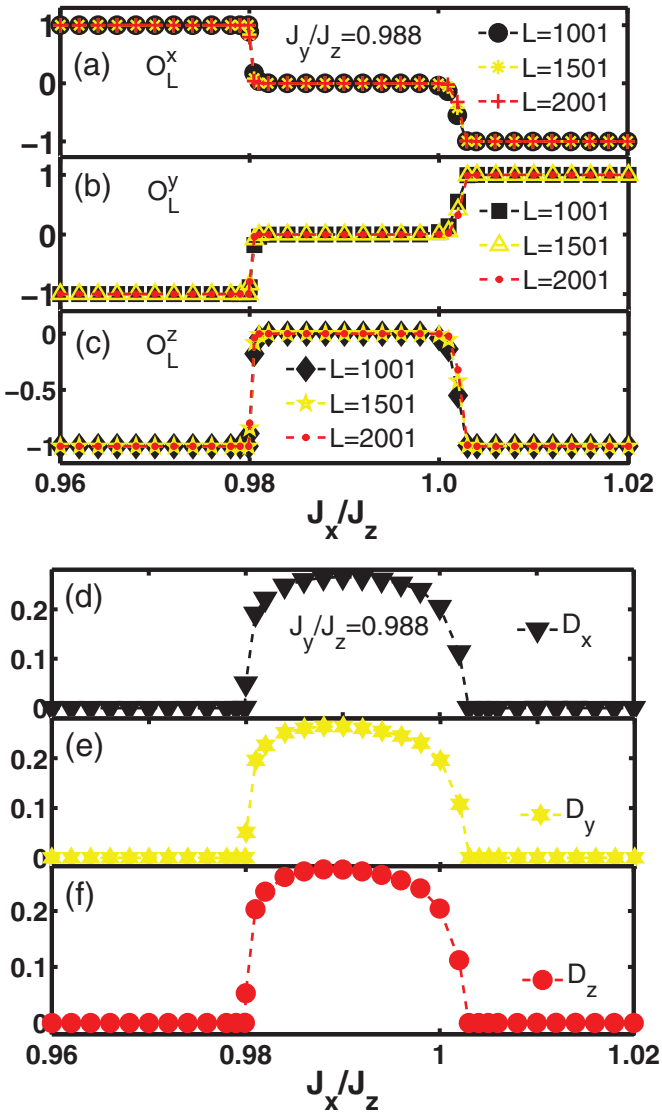

FIG. 4. (Top) Non-local- and (bottom) local-order parameters as a function of control parameter J_x/J_z with truncation dimension $\chi = 100$ for fixed $J_y/J_z = 0.988$. Two QPT points are detected at $J_x^{c_1}/J_z = 0.9799$ and $J_x^{c_2}/J_z = 1.003$. Here, $\boldsymbol{K} = (1, -1, -1)$ on the left-hand side of $J_x^{c_1}/J_z$ and $\boldsymbol{K} = (-1, 1, -1)$ on the right-hand side of $J_x^{c_2}/J_z$. In the region between $J_x^{c_1}/J_z$ and $J_x^{c_2}/J_z$, $\boldsymbol{K} = (0, 0, 0)$ where the dimerized phase is characterized by the combined local order parameter $\boldsymbol{D} = (D_x, D_y, D_z)$. The data sets correspond to line (iii) in Fig. 1(b).

dimension $\chi = 100$ in Fig. 4. Here, two QPT points are located at $J_x^{c_1}/J_z = 0.9799$ and $J_x^{c_2}/J_z = 1.003$. The SPt phase on the left-hand side of $J_x^{c_1}/J_z$ corresponding to PA is characterized by $\boldsymbol{K} = (1, -1, -1)$. The SPt phase on the right-hand side of $J_x^{c_2}/J_z$ corresponding to PB is characterized by $\boldsymbol{K} = (-1, 1, -1)$. We note that the saturation rate of O_L^x, O_L^y, and O_L^z at $J_x^{c_1}/J_z = 0.9799$ and $J_x^{c_2}/J_z = 1.003$ is much slower than the rate at $J_y^c/J_z = 0.4$ and 0.6.

VI. DIMERIZED PHASE

We, now, concentrate on the dimerized phase in the vicinity of the isotropic point $J_x = J_y = J_z$ for which long-range order exists. With fixed $J_y/J_z = 0.988$, SSB occurs when control parameter J_x/J_z crosses the points $J_x^{c_1}/J_z = 0.9799$ and $J_x^{c_2}/J_z = 1.003$. To characterize the long-range order in the region between these two points, we consider dimerized local order parameter $\langle S_i S_{i+1} - S_{i+1} S_{i+2} \rangle$ [5]. Unfortunately, this definition only fits the system with SU(2) symmetry. However, a systematic method based on tensor network representations to derive local-order parameters has been established [15]. Following this method, we analyze the combined dimerized local-order parameters $\boldsymbol{D} = (D_x, D_y, D_z)$, with $D_\alpha = \langle S_i^\alpha S_{i+1}^\alpha - S_{i+1}^\alpha S_{i+2}^\alpha \rangle$. Figure 4 shows plots of these dimerized local-order parameters as a function of control parameter J_x/J_z with truncation dimension $\chi = 100$ for fixed $J_y/J_z = 0.988$. The dimerized long-range-order $\boldsymbol{D}$ is clearly evident between $J_x^{c_1}/J_z = 0.9799$ and $J_x^{c_2}/J_z = 1.003$. Figure 4 clearly demonstrates the complementarity between the local- and non-local-order parameters.

VII. VON NEUMANN ENTROPY AND CENTRAL CHARGE

To examine the nature of the QPT between SPt and dimerized phases, we first discuss the definition of von Neumann entropy as a measure of bipartition entanglement. Consider state $|\psi\rangle$ as being composed of two semi-infinite chains $L(-\infty, \ldots, i)$ and $R(i+1, \ldots, +\infty)$, connected by the Schmidt decomposition coefficient λ_α. This implies $|\psi\rangle$ can be expressed as $|\psi\rangle = \sum_{\alpha=1}^{\chi} \lambda_\alpha |\phi_\alpha^L\rangle |\phi_\alpha^R\rangle$, where $|\phi_\alpha^L\rangle$ and $|\phi_\alpha^R\rangle$ are the Schmidt bases of the two semi-infinite chains L and R. Consequently, the von Neumann entropy can be defined as [16] $S = -\mathrm{Tr}\, \rho_L \ln \rho_L = -\mathrm{Tr}\, \rho_R \ln \rho_R$, where $\rho_L = \mathrm{Tr}_R\, \rho$ and $\rho_R = \mathrm{Tr}_L\, \rho$ are the reduced matrices of the subsystems of L and R, respectively, with density matrix $\rho = |\phi\rangle\langle\phi|$. For the semi-infinite chains L and R of iMPS, the von Neumann entropy S is written as

$$S = -\sum_{\alpha=1}^{\chi} \lambda_\alpha^2 \ln \lambda_\alpha^2. \tag{4}$$

At a critical point in a one-dimensional system, the semilogarithmic scaling of the von Neumann entropy versus truncation dimension χ follows from conformal invariance with scaling ruled by the central charge of the underlying conformal field theory. In addition, the correlation length ξ of the iMPS exhibits a power scaling with truncation dimension χ. These two scaling relations can be written as [17–20]

$$S_\chi \propto \frac{c\kappa}{6} \ln \chi, \qquad \xi_\chi \propto \xi_0\, \chi^\kappa. \tag{5}$$

Here, c denotes the central charge, and κ is a finite entanglement scaling exponent. ξ_0 is a constant. For a given χ, the correlation length ξ can be obtained by the largest and the second largest eigenvalues $D_0(\chi)$ and $D_1(\chi)$ of the transfer matrix with $\xi_\chi = 1/\ln |D_0(\chi)/D_1(\chi)|$. By making use of the relations (5), one can obtain numerical estimates for the central charge on the phase boundary between SPt phases and between SPt and dimerized phases.

For this purpose, we choose $J_y/J_z = 0.4$ with fixed $J_x^c/J_z = 0.4$ and choose $J_y/J_z = 1$ with QPT points J_x^c/J_z ranging from 0.986 30 to 0.98 804 as the truncation dimension χ increases from 75 to 600. Figure 5 shows a corresponding plot of the von Neumann entropy and correlation length as

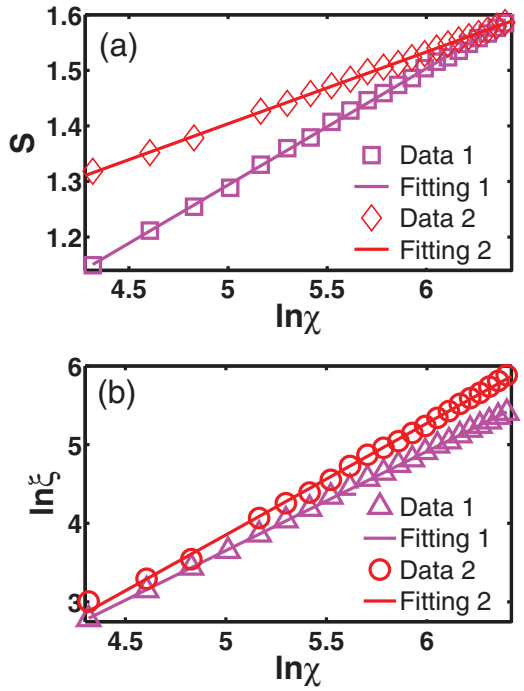

FIG. 5. The scaling of (a) von Neumann entropy S and (b) correlation length ξ with the truncation dimension χ. (i) For fixed $J_x/J_z = 0.4$ with $J_y^c/J_z = 0.4$, shown in purple and labeled as Fitting 1, the central charge is estimated to be $c_1 = 0.997$. (ii) For fixed $J_y/J_z = 1$ with QPT points J_x^c/J_z ranging from 0.986 30 to 0.988 04 as the truncation dimension χ increases from 75 to 600, shown in red and labeled as Fitting 2, the central charge is estimated to be $c_2 = 0.5463$.

a function of truncation dimension χ ranging from 75 to 600. Both the von Neumann entropy and correlation length diverge with increasing truncation dimension χ. To extract the central charge, we use the fitting functions $S_\chi = \frac{c\kappa}{6} \ln \chi + a$ and $\ln \xi_\chi = \kappa \ln \chi + b$ and consider two cases. (i) For the case of fixed $J_x/J_z = 0.4$ with $J_y^c/J_z = 0.4$, shown in purple in Fig. 5 and labeled as Fitting 1, the fitting coefficients are given by $c_1\kappa_1/6 = 0.209\,68$, $a_1 = 0.245\,27$, $b_1 = -2.6563$, and $\kappa_1 = 1.2619$. The central charge is estimated to be $c_1 = 0.997$. This is consistent with a general argument that a phase transition between SPt phases belongs to the Gaussian universality class [2]. (ii) For the case of fixed $J_y/J_z = 1$ with QPT points J_x^c/J_z ranging from 0.986 30 to 0.988 04 as the truncation dimension χ increases from 75 to 600, shown in red in Fig. 5 and labeled as Fitting 2, the fitting coefficients are given by $c_2\kappa_2/6 = 0.129\,29$, $a_2 = 0.757\,42$, $b_2 = -3.2471$, and $\kappa_2 = 1.4199$. As a result, the central charge is estimated to be $c_2 = 0.5463$. This indicates that the phase transition falls into the Ising universality class as anticipated from the fact that a Z_2 symmetry is spontaneously broken in the dimerized phase.

VIII. SUMMARY

We have investigated the nature of quantum SPt phases and quantum phase transitions in the spin-1 antiferromagnetic anisotropic biquadratic model (1) by making use of quantum duality and symmetry transformations, along with iTEBD and iDMRG algorithms. The concept of SPt phases, originally defined through the combined operation of the site-centered inversion with the π rotation around the z axis in the spin space [2] is extended in order to keep consistency with the duality transformations, which themselves are induced from the symmetric group S_3 with respect to x, y, and z.

The ground-state phase diagram in Fig. 1(b) has been determined by studying the principal regime, which can be mapped to the other five regions of the phase diagram via the quantum duality and symmetry transformations summarized in Table I. The phase boundaries are determined by calculating the non-local- and local-order parameters of the principal regime. To illustrate our strategy, three sample lines, $J_x/J_z = 0.4$, $J_x/J_z = 0.6$, and $J_y/J_z = 0.988$ are studied in detail. The phase diagram is shown to be composed of four phases characterized by the non-local-order parameters $\boldsymbol{K} = (1, -1, -1)$, $\boldsymbol{K} = (-1, 1, -1)$, and $\boldsymbol{K} = (-1, -1, 1)$, and a combined dimerized local-order parameter. In addition, the von Neumann entropy and correlation length have been used to estimate the central charge $c = 0.5463$ on the boundary between SPt and dimerized phases. This value is suggestive of the Ising-type universality class. The central charge value of $c = 0.997$ is extracted on the phase boundary between SPt phases, corresponding to the Gaussian-type universality class. We have also identified three characteristic lines of factorized ground states, which are located in the SPt phases instead of a symmetry-breaking phase, in sharp contrast to other known cases [21,22]. Our results suggest the importance and potential generality of SPt phases in a classification of quantum states of matter.

ACKNOWLEDGMENTS

I.M. acknowledges support from the ARC Future Fellowships scheme, Grant No. FT140100625. The work of M.T.B. has been supported by the National Natural Science Foundation of China Grant No. 11575037 and Australian Research Council Discovery Project No. DP180101040.

[1] X. Chen, Z.-C. Gu, and X.-G. Wen, Phys. Rev. B **83**, 035107 (2011); **84**, 235128 (2011).

[2] Y. Fuji, F. Pollmann, and M. Oshikawa, Phys. Rev. Lett. **114**, 177204 (2015).

[3] A. Kshetrimayum, H.-H. Tu, and R. Orús, Phys. Rev. B **93**, 245112 (2016).

[4] H.-Q. Zhou, Q.-Q. Shi, and Y.-W. Dai, arXiv:1709.09838; Q.-Q. Shi, S.-H. Li, and H.-Q. Zhou, J. Phys. A: Math. Theor. **53**, 155301 (2020).

[5] M. N. Barber and M. T. Batchelor, Phys. Rev. B **40**, 4621 (1989).
[6] A. Klümper, Europhys. Lett. **9**, 815 (1989); J. Phys. A **23**, 809 (1990).
[7] R. J. Baxter, *Exactly Solved Models in Statistical Mechanics* (Dover, New York, 2008).
[8] I. Affleck, J. Phys.: Condens. Matter **2**, 405 (1990).
[9] G. Vidal, Phys. Rev. Lett. **98**, 070201 (2007).
[10] I. P. McCulloch, arXiv:0804.2509.
[11] O. A. Castro-Alvaredo and B. Doyon, Phys. Rev. Lett. **108**, 120401 (2012).
[12] J. Haegeman, D. Perez-Garcia, I. Cirac, and N. Schuch, Phys. Rev. Lett. **109**, 050402 (2012).
[13] N. Schuch, D. Perez-Garcia, and I. Cirac, Phys. Rev. B **84**, 165139 (2011).
[14] For a similar definition of bond-centered non-local-order parameters, see F. Pollmann, and A. M. Turner, Phys. Rev. B **86**, 125441 (2012).
[15] H.-Q. Zhou, arXiv:0803.0585.
[16] C. H. Bennett, H. J. Bernstein, S. Popescu, and B. Schumacher, Phys. Rev. A **53**, 2046 (1996).
[17] V. E. Korepin, Phys. Rev. Lett. **92**, 096402 (2004); P. Calabrese and J. Cardy, J. Stat. Mech.: Theory Exp. (2004) P06002.
[18] L. Tagliacozzo, T. R. de Oliveira, S. Iblisdir, and J. I. Latorre, Phys. Rev. B **78**, 024410 (2008).
[19] F. Pollmann, S. Mukerjee, A. M. Turner, and J. E. Moore, Phys. Rev. Lett. **102**, 255701 (2009).
[20] Y.-W. Dai, B.-Q. Hu, J.-H. Zhao, and H.-Q. Zhou, J. Phys. A: Math. Theor. **43**, 372001 (2010).
[21] S. M. Giampaolo, G. Adesso, and F. Illuminati, Phys. Rev. Lett. **100**, 197201 (2008); Phys. Rev. B **79**, 224434 (2009); Phys. Rev. Lett. **104**, 207202 (2010).
[22] J. Kurmann, H. Thomas, and G. Muller, Physica A (Amsterdam) **112**, 235 (1982); T. Roscilde, P. Verrucchi, A. Fubini, S. Haas, and V. Tognetti, Phys. Rev. Lett. **93**, 167203 (2004); **94**, 147208 (2005).